Published in final edited form as:
IEEE Trans Biomed Circuits Syst. 2008 September 1; 2(3): 204–211. doi:10.1109/TBCAS.2008.2003195.

Development of a Time Domain Fluorimeter for Fluorescent Lifetime Multiplexing Analysis

Christopher D. Salthouse, **Ralph Weissleder**, and **Umar Mahmood**
Center for Molecular Imaging Research (CMIR), the Massachusetts General Hospital, Charlestown, MA 02129-2060 USA

Christopher D. Salthouse: csalthouse@mgh.harvard.edu; Ralph Weissleder: ; Umar Mahmood:

Abstract

We show that a portable, inexpensive USB-powered time domain fluorimeter (TDF) and analysis scheme were developed for use in evaluating a new class of fluorescent lifetime multiplexed dyes. Fluorescent proteins, organic dyes, and quantum dots allow the labeling of more and more individual features within biological systems, but the wide absorption and emission spectra of these fluorophores limit the number of distinct processes which may be simultaneously imaged using spectral separation alone. By additionally separating reporters in a second dimension, fluorescent lifetime multiplexing provides a means to multiply the number of available imaging channels.

Index Terms

Analog circuits; biomedical imaging; fluorescence; optical pulses

I. Introduction

Fluorophores are used as probes in biomedical imaging systems because the light they emit can be detected even at very low probe concentrations. Small-molecule fluorophores and quantum dots are both used as externally administered probes. The fluorophores are attached to a targeted molecule such as an antibody fragment that allows the probe to label biological processes. In animal research, fluorescent proteins (FPs) offer a complimentary approach to labeling. The DNA corresponding to the FP can be inserted into the genome following specific promoters so that the FP is only generated in specific cell types [1], [2].

Despite the large number of fluorophores available (1300 fluorophore spectra are collected in one archive alone [3]) the number of independent fluorescent channels is relatively small because the wide absorption and emission spectra of fluorophores limit the number of independent spectral channels. Fig. 1(a) demonstrates the high degree of spectral overlap for a collection of small molecule fluorophores. Fig. 1(b) demonstrates that the addition of a fluorescent lifetime dimension adds to the separation between the fluorophores. This can increase the total number of imaging channels. As a first step towards the multiplicative increase in the number of imaging channels by three or four suggested by Fig. 1, this paper demonstrates the separation of fluorescence from two fluorophores in the same spectral window.

Correspondence to: Christopher D. Salthouse, csalthouse@mgh.harvard.edu.

Time domain separation is based on a property of fluorophores called fluorescent lifetime, a measure of the temporal response of fluorophores to pulsed excitation. A theoretical time response of two fluorophores is shown in Fig. 2. The excitation pulse is short in duration. The fluorophores are excited by the pulse and then decay, emitting photons, with a constant probability of decay for each excited fluorophore. This constant probability of decay from a decreasing population leads to the characteristic exponential decay of fluorescence intensity

$$p(t)=e^{-t/\tau}. \tag{1}$$

The fluorescent lifetime of a fluorophore τ is a property of the fluorophore distinct from its absorption and emission spectral properties. As with absorption and emission spectra, fluorescent lifetimes of some fluorophores are sensitive to environmental conditions including pH and temperature. Other fluorophores are relatively insensitive to environmental conditions and show little change in fluorescent lifetimes. Fluorescent lifetime measurements are useful for both types of fluorophores.

Instruments to measure fluorescent lifetime have been built using a variety of technologies including: direct digitization systems, time correlated single photon counting (TCSPC) systems, streak cameras, and gated optical intensifiers. Spot measurements can be made in two ways. The fluorescence can be digitized directly using a high-bandwidth oscilloscope and sensor such as a photodiode or photomultiplier tube, or the arrival time of individual photons can be digitizing using special single photon sensors in TCSPC [5], [6]. Measurements can be made of a line at a time using streak cameras. A slit of light is converted into electrons by a photocathode and the electrons are deflected by a time varying electric field such that the image captured by a CCD of the electrons hitting a phosphor screen contains spatial information in one dimension and temporal information in the other [7]. Two-dimensional images can be captured with high temporal resolution using a gated optical intensifier acting as a shutter for the subnanosecond exposures required to measure fluorescent lifetimes of many fluorophores [8].

It is possible to make measurements more quickly in cases where there is *a priori* information about the fluorescent lifetime. When each point contains only a single fluorescent species with a single exponential decay, then rapid lifetime determination (RLD) may be used to measure the lifetime based on the fluorescence intensity in two time windows [9].

Because of the unique properties of an exponential, RLD can be used to determine fluorescent lifetime independent of excitation pulse width. The fluorescence signal $F(t)$, is the convolution of the excitation pulse $E(i)$, and the impulse response of the fluorophore $I(t)$

$$I(t)=Ae^{-t/\tau} \tag{2}$$

$$F(t)=E(t)*I(t)=\int_{a=0}^{a=t}E(a)I(t-a)da. \tag{3}$$

RLD can be used to calculate the fluorescent lifetime by integrating the fluorescence in two windows of length t_{win} following the end of the excitation pulse at t_1

$$\tau_{\mathrm{RLD}}=\frac{-t_{\mathrm{win}}}{\ln\left(\frac{\int_{t=t_1+t_{\mathrm{win}}}^{t=t_1+2t_{\mathrm{win}}}F(t)dt}{\int_{t=t_1}^{t=t_1+t_{\mathrm{win}}}F(t)dt}\right)}. \tag{4}$$

The $F(t)$ term can be expanded using (2) and (3)

$$\tau_{\mathrm{RLD}}=\frac{-t_{\mathrm{win}}}{\ln\left(\frac{\int_{t=t_1+t_{\mathrm{win}}}^{t=t_1+2t_{\mathrm{win}}}\int_{a=0}^{a=t}E(a)Ae^{-(t-a)/\tau}dadt}{\int_{t=t_1}^{t=t_1+t_{\mathrm{win}}}\int_{a=0}^{a=t}E(a)Ae^{-(t-a)/\tau}dadt}\right)}. \tag{5}$$

Because the excitation has ended before either integration windows begins, the integrals can be rearranged to separate the variables a and t

$$\tau_{\mathrm{RLD}}=\frac{-t_{\mathrm{win}}}{\ln\left(\frac{\int_{t=t_1+t_{\mathrm{win}}}^{t=t_1+2t_{\mathrm{win}}}e^{-t/\tau}dt\int_{a=0}^{a=t_1}E(a)Ae^{a/\tau}da}{\int_{t=t_1}^{t=t_1+t_{\mathrm{win}}}e^{-t/\tau}dt\int_{a=0}^{a=t_1}E(a)Ae^{a/\tau}da}\right)}. \tag{6}$$

The excitation terms cancel out and the calculated time constant agrees with the fluorescent lifetime

$$\tau_{\mathrm{RLD}}=\frac{-t_{\mathrm{win}}}{\ln\left(e^{-t_{\mathrm{win}}/\tau}\right)}=\tau. \tag{7}$$

So, the temporal resolution of the instrument is not limited by the width or shape of the excitation pulse. The most important characteristic of an excitation pulse is a fast fall-edge transition to maximize the fluorescence measured after the end of the excitation pulse.

II. Fluorescent Lifetime Multiplexing

Fluorescent lifetime multiplexing is the independent measurement of fluorescence intensity from two fluorophores based on fluorescent lifetime. A mathematical framework for fluorescent lifetime multiplexing has been previously reported [10], in this work we are demonstrating that fluorescent lifetime multiplexing can be performed on two fluorophores with known single-exponential fluorescent lifetimes using only fluorescence intensity measurements from two time windows. We have developed an inexpensive sensor and a novel analysis method capable of measuring these two fluorescence intensities within a single spectral window.

In the special case where appropriate fluorescent lifetimes and intensities are chosen, the fluorescent intensity from two fluorophores can be determined graphically from a plot of combined fluorescence versus time as shown in Fig. 3. Taking the logarithm of the intensity turns the individual exponential decays into straight lines. For this special case, the combined fluorescent decay has two straight slopes corresponding to the fluorescent lifetimes of the two

fluorophores. The fluorescence from each of the two fluorophores can be seen graphically as the extension of the corresponding slopes.

In general, the fluorescence decay of a mixture of two fluorophores does not contain regions with linear slopes in a semilog plot, in this case the two amplitudes can be solved algebraically if the two fluorescent lifetimes are known. The fluorescence from each fluorophore as a function of time is

$$F_1(t)=A_1e^{-t/\tau_1} \qquad F_2(t)=A_2e^{-t/\tau_2}. \tag{2a}$$

The total fluorescence in window one from the end of excitation $t = 0$ to $t = t_{\text{win}}$ is

$$\begin{aligned} F_{\text{win1}} &= \int_0^{t_{\text{win}}} A_1e^{-t/\tau_1}\,dt + \int_0^{t_{\text{win}}} A_2e^{-t/\tau_2}\,dt \\ &= -A_1\tau_1e^{-t/\tau_1}\Big]_0^{t_{\text{win}}} - A_2\tau_2e^{-t/\tau_2}\Big]_0^{t_{\text{win}}} \\ &= A_1\tau_1 - A_1\tau_1e^{-t_{\text{win}}/\tau_1} + A_2\tau_2 - A_2\tau_2e^{-t_{\text{win}}/\tau_2} \\ &= A_1\tau_1\left(1-e^{-t_{\text{win}}/\tau_1}\right) + A_2\tau_2\left(1-e^{-t_{\text{win}}/\tau_2}\right). \end{aligned} \tag{3a}$$

The total fluorescence in window two from the end of window one to $t = 2t_{\text{win}}$ is

$$\begin{aligned} F_{\text{win2}} &= \int_{t_{\text{win}}}^{2t_{\text{win}}} A_1e^{-t/\tau_1}\,dt + \int_{t_{\text{win}}}^{2t_{\text{win}}} A_2e^{-t/\tau_2}\,dt \\ &= -A_1\tau_1e^{-t/\tau_1}\Big]_{t_{\text{win}}}^{2t_{\text{win}}} - A_2\tau_2e^{-t/\tau_2}\Big]_{t_{\text{win}}}^{2t_{\text{win}}} \\ &= A_1\tau_1e^{-t_{\text{win}}/\tau_1} - A_1\tau_1e^{-2t_{\text{win}}/\tau_1} \\ &\quad + A_2\tau_2e^{-t_{\text{win}}/\tau_2} - A_2\tau_2e^{-2t_{\text{win}}/\tau_2} \\ &= A_1\tau_1e^{-t_{\text{win}}/\tau_1}\left(1-e^{-t_{\text{win}}/\tau_1}\right) \\ &\quad + A_2\tau_2e^{-t_{\text{win}}/\tau_2}\left(1-e^{-t_{\text{win}}/\tau_2}\right). \end{aligned} \tag{4a}$$

Then the equations are solved for the two amplitudes, as shown in (5a)–(9) at the bottom of the page.

The calculation of the pre-exponential factors A_1 and A_2 is sensitive to noise in the fluorescence signal measured in the two time-gates as shown in (8) and (9). Errors in the pre-exponential factors can also be introduced by errors in the estimated fluorescent lifetimes of the fluorophores ($\tau_{1,\text{est}}$ and. $\tau_{2,\text{est}}$) as compared to the actual fluorescent lifetimes (τ_1 and τ_2) or in the estimate of the integration window length ($t_{\text{win,est}}$) as compared to the actual integration window length (t_{win}). The sensitivity to these parameter estimation errors are calculated by substituting (3a) and (4a) back into (8) and (9) to form (10) and (11), as shown at the bottom of the page.

The effect of parameter variation is plotted in Fig. 4. The fluorescent lifetimes were chosen to be 2 and 4 ns with a 3-ns integration time window for this simulation. Each parameter was then varied from 20% below to 20% above the actual value. A low estimate of τ_2 has the greatest effect, with up to a 60% error in calculated fluorescence intensity from a 20% error in fluorescent lifetime. The other parameters cause a maximum error of less than 30% across the variation range.

III. Time Domain Fluorimeter (TDF) Design

We present a novel TDF designed for in vitro fluorescent lifetime multiplexing such as the development of multiplex imaging agents. The TDF measures fluorescence in a time window. The FWHM width of the window is adjusted with 250-ps time resolution so that appropriate integration windows can be chosen where the fluorescence decay fits within the dynamic range of the system. For example, when multiplexing dyes with 1- and 2-ns fluorescent lifetimes, 2-ns windows will ensure than even in a solution with only the 1-ns dye present, the fluorescence recorded in the second window will be only an order of magnitude less than in the first window. To minimize the reagent requirements for experimental compounds, the TDF is optimized for sensing 50 μL of 5-μM dye solution in a standard low volume cuvette. For ease of use, the device is powered and interfaced to a personal computer through a universal serial port (USB).

$$A_2=\frac{F_{\text{win1}}-A_1\tau_1(1-e^{-t_{\text{win}}/\tau_1})}{\tau_2(1-e^{-t_{\text{win}}/\tau_2})} \tag{5a}$$

$$F_{\text{win2}}=A_1\tau_1 e^{-t_{\text{win}}/\tau_1}\left(1-e^{-t_{\text{win}}/\tau_1}\right)+\frac{F_{\text{win1}}-A_1\tau_1(1-e^{-t_{\text{win}}/\tau_1})}{\tau_2(1-e^{-t_{\text{win}}/\tau_2})}\tau_2 e^{-t_{\text{win}}/\tau_2}\left(1-e^{-t_{\text{win}}/\tau_2}\right) \tag{6a}$$

$$F_{\text{win2}}-F_{\text{win1}}e^{-t_{\text{win}}/\tau_2}=A_1\tau_1\left(1-e^{-t_{\text{win}}/\tau_1}\right)\left(e^{-t_{\text{win}}/\tau_1}-e^{-t_{\text{win}}/\tau_2}\right) \tag{7a}$$

$$A_1=\frac{F_{\text{win2}}-F_{\text{win1}}e^{-t_{\text{win}}/\tau_2}}{\tau_1(1-e^{-t_{\text{win}}/\tau_1})(e^{-t_{\text{win}}/\tau_1}-e^{-t_{\text{win}}/\tau_2})} \tag{8}$$

$$\begin{aligned}A_2&=\frac{F_{\text{win1}}-\frac{F_{\text{win2}}-F_{\text{win1}}e^{-t_{\text{win}}/\tau_2}}{\tau_1(1-e^{-t_{\text{win}}/\tau_1})(e^{-t_{\text{win}}/\tau_1}-e^{-t_{\text{win}}/\tau_2})}\tau_1(1-e^{-t_{\text{win}}/\tau_1})}{\tau_2(1-e^{-t_{\text{win}}/\tau_2})}\\&=\frac{F_{\text{win1}}\tau_1 e^{-t_{\text{win}}/\tau_1}(1-e^{-t_{\text{win}}/\tau_1})-F_{\text{win2}}\tau_1(1-e^{-t_{\text{win}}/\tau_1})}{\tau_1(1-e^{-t_{\text{win}}/\tau_1})(e^{-t_{\text{win}}/\tau_1}-e^{-t_{\text{win}}/\tau_2})\tau_2(1-e^{-t_{\text{win}}/\tau_2})}\\&=\frac{F_{\text{win1}}e^{-t_{\text{win}}/\tau_1}-F_{\text{win2}}}{\tau_2(1-e^{-t_{\text{win}}/\tau_2})(e^{-t_{\text{win}}/\tau_1}-e^{-t_{\text{win}}/\tau_2})}\end{aligned} \tag{9}$$

$$A_{1,calc}=\frac{[(A_1\tau_1(1-e^{-t_{\text{win}}/\tau_1})(e^{-t_{\text{win}}/\tau_1}-e^{-t_{\text{win}}/\tau_{2,\text{est}}}))-(A_2\tau_2(1-e^{-t_{\text{win}}/\tau_2})(e^{-t_{\text{win}}/\tau_2}-e^{-t_{\text{win}}/\tau_{2,\text{est}}}))]}{\tau_{1,\text{est}}(1-e^{-t_{\text{win,est}}/\tau_{1,\text{est}}})(e^{-t_{\text{win,est}}/\tau_{1,\text{est}}}-e^{-t_{\text{win,est}}/\tau_{2,\text{est}}})} \tag{10}$$

$$A_{2,calc}=\frac{[(A_1\tau_1(1-e^{-t_{\text{win}}/\tau_1})(e^{-t_{\text{win}}/\tau_{1,\text{est}}}-e^{-t_{\text{win}}/\tau_1}))+(A_2\tau_2(1-e^{-t_{\text{win}}/\tau_2})(e^{-t_{\text{win}}/\tau_{1,\text{est}}}-e^{-t_{\text{win}}/\tau_2}))]}{\tau_{2,\text{est}}(1-e^{-t_{\text{win,est}}/\tau_{2,\text{est}}})(e^{-t_{\text{win,est}}/\tau_{1,\text{est}}}-e^{-t_{\text{win,est}}/\tau_{2,\text{est}}})}. \tag{11}$$

As shown in Fig. 5, our TDF consists of five building blocks for measuring the fluorescence lifetime of a small sample. Following a trigger pulse from the timing circuit, the excitation circuit emits a high-power laser pulse lasting a few nanoseconds. This pulse generates

fluorescence in the sample. The integrating sensor then integrates between reset pulses. The output of the integrating sensor is digitized in the microcontroller and sent over the USB to the computer. The fluorescence within specific time windows is measured by taking the difference between two integrated windows. First, the delay between the trigger and reset pulses is set so that the reset ends at the beginning of the desired window. The integrating sensor then measures the total fluorescence from the beginning of the window until the end of the fluorescence. Then, the delay is set so that the end of the reset corresponds to the end of the desired window. The integrating sensor then measures the total fluorescence from the end of the desired window until the end of the pulse. The difference between these two measurements is the fluorescence in the desired time window.

A. Excitation Circuit

The high-intensity focused excitation beam is provided by a 90-mW, 658-nm laser diode (Thorlabs HL6535MG) originally designed for use in a DVD writer. The laser is collimated using a US-Lasers 6.4-mm housing kit to a 1-mm-wide beam for the 1-cm path through the cuvette. The laser diode is driven by a group of four nMOS power transistors (Digikey 568-1974-2-ND) with a pulse from the timing circuit as shown in Fig. 5. The power transistors conduct as their gates are raised towards the supply voltage. At the end of the pulse, the gate of the transistor is pulled to ground. The source voltage is pulled down by the laser diode, but the transistor remains back biased by approximately half a volt. This reverse bias overcomes the 10-μA zero-bias transmission of the transistor. Despite the 500-mA rated current of the transistor, four transistors are ganged in parallel to obtain the necessary 100-mA peak current in this short-pulsed configuration.

B. Integrating Sensor Circuit

Even with the bright excitation signal produced by the excitation circuit, the measured fluorescence is still very low primarily because of the omni directional radiation of fluorescence and the limited collection angle of available high-temporal-resolution imaging sensors. A Hamamatsu S2382 avalanche photodiode (APD) with an active area of 0.19 mm^2 was chosen because of its 900 MHz cut-off frequency. In the TDF, the photodiode is placed just 2 mm from the sample in the cuvette and 3.5 mm from the center of the excitation beam.

The APD reaches maximum amplification before long transients interfere with measurements with 182 V of back bias supplied by a dc-dc step up converter (EMCO G05).

Fig. 7 shows the APD along with amplification circuitry. The amplified photo current charges the parasitic capacitance at node A. The temporal response of the sensing circuit comes from the reset transistor that discharges the parasitic capacitance at node A. An 8-ns reset pulse is sent from the timing circuitry. The delay between the laser excitation and the reset pulse is varied to sample different portions of the fluorescent decay. The additional capacitance at the input of the operational amplifier is not discharged by the reset because of the 1-MOhm resistor, maximizing the current-to-voltage conversion efficiency. A 1-pa-input-current operational amplifier (Analog Devices AD8662) is used for the initial buffering so that the maximum error from current flow through the 1-MOhm resistor is limited to below 1 μV.

Charge injection is a significant source of error in these measurements, so a dummy switch is also used. The dummy voltage at node B is subtracted from the signal voltage using a standard resistor-op-amp subtracter. A second stage then inverts this signal and offers the option of additional gain that was not used in this application. Finally, a low pass filter removes remaining switching artifacts and averages over multiple excitations prior to digitization.

C. Timing Circuit

The timing circuit begins with a ring oscillator built out of three inverters (74HC04AFN) in Fig. 8. The oscillation frequency is lowered from 20 MHz to 850 kHz with the addition of a 47-k Ohm resistor and 10-pF capacitor in order to allow enough time between excitations to measure long fluorescent lifetimes. The oscillator output is then split into two paths leading to the excitation and sensing circuits. The excitation input is further delayed by a few nanoseconds using a resistance-capacitance (*RC*) delay formed by a discrete resistor and the parasitic capacitance of the input of an inverter gate. The reset signal for the integrating sensor is delayed through a programmable digital delay line (Dallas Semiconductor DS1021-25). The delay is adjustable in 250-ps steps with the delay value set by the microcontroller.

The drive pulses for both the reset and the excitation are generated from square waves using inverters along with a resistor-capacitor pulse shaper. The falling edge at the input to C_{ex} lowers the voltage at node *X,* causing the trigger signal to rise high. Node *X* is then charged through R_{ex}. When it reaches half of the supply voltage, at approximately $0.69R_{\mathrm{ex}}C_{\mathrm{ex}}$, the output trigger signal returns to ground. The circuit was constructed using a 560 Ohm resistor and a variable capacitor that varies between 7.5 pF and 30 pF (Digikey SG2039CT-ND) for manual adjustment from 4 to 17 ns.

D. Microcontroller

The circuitry is interfaced to a computer through a microcontroller (Microchip PIC 18f4550). It programs the digital delay line through a serial bus and digitizes the output of the integrating sensor with a integrated 10-bit analog-to-digital converter. The computer communicates with the microcontroller over a USB connection presented to software applications through a serial port emulator. The microcontroller responds to two commands: a delay set and a data request. The delay command sets the bits to vary the digital delay in the timing circuit. The microcontroller responds to data requests by digitizing the output of the sensing module and averaging 100 digitizations and reporting that value.

E. Software

The software running on a personal computer serves as both a data recording system and a debugging interface. In scan mode, the software steps through each delay value from 0 to 30 ns and records the corresponding data point to a comma-separated-value data file for further processing in Excel or Matlab. A new file is created for each scan. In debug mode, commands typed into the text window are forwarded to the microcontroller and log of the serial communications is displayed.

F. Mechanical System

The TDF is a portable USB powered device enclosed in a 4 in by 6 in plastic box. Inside the box are two circuit boards as shown in Fig. 8(a). The first board contains the power supply for the avalanche photo diode. The second board, Fig. 8(b), contains the remaining custom circuitry. The black cuvette holder supports a microcuvette with a 10 mm by 2 mm sample chamber. The laser travels the full length of the 10-mm sample. The photodiode is placed along the side of the channel perpendicular to the laser path to maximize the fluorescence signal collected while minimizing the collection of excitation photons. Because this system is designed to measure only temporal effects, no spectral filters are used.

IV. Results

The TDF was tested starting the excitation block and adding blocks one at a time. First, the excitation pulse was measured using a photodiode and a gigahertz oscilloscope. Then, the

temporal accuracy of the system was verified by measuring the excitation pulse with the detector. The sensitivity was then tested by using the system to measure the fluorescence lifetime of dye in solution. Finally, the multiplexing was demonstrated by measuring mixtures of two fluorophores with known concentrations.

A. Excitation

The excitation pulse was measured using an avalanche photodetector with 100 V of back bias. The shape of the optical pulses is measured using a 1-GHz oscilloscope. Adjusting the electrical trigger pulse width from 4 to 11 ns varied the optical pulse from 2 to 9 ns. The integrated optical power of the laser pulse was measured using an optical power meter (Edmund Optics Lasercheck.) The integrated power was combined with the waveform shape to generate the curves in Fig. 10, which demonstrates a peak power of over 100 mW for a 9-ns pulse and decreasing peak power for shorter pulses.

B. Sensing Circuit

By bouncing the excitation off of a piece of paper, we were able to measure the excitation pulse using the TDF measurement circuits. The delay value was set to each value between 0 and 11 ns generating the curves in Fig. 11 for the same excitation pulse lengths used in Fig. 10. Each data point was averaged 100 times in the microcontroller. The software then averaged over 100 sweeps collected over 12 min of acquisition. Inside the circuit, the raw signal at node A of the integrating sensor varies from 3.3 to 2.4 V. The gain of 2.5 on the subtracter amplifies the signal swing to 1.35 to 3.6 V.

C. Measuring Fluorescent Lifetime

The system was then used to measure the fluorescent lifetime of individual fluorophores. Three commercially available organic dyes with matched absorption and emission spectra and published single exponential fluorescent lifetimes were used: Cy5, ATTO 647, and ATTO 647N. The fluorophores have maximum absorption at 647, 645, and 644 nm, respectively, and an emission peaks at 666, 669, and 669 nm, respectively. This system places the detector as close to the sample as possible to maximize the amount of fluorescence detected. This leaves no space for a spectral filter, so the measured signal includes components from fluorescence and excitation light that is scattered by the sample into the detector. The single exponential decay shown as straight lines in Fig. 12 and the agreement between previously published fluorescent lifetime values and measurements made with this device demonstrate that the fluorescence signal predominates for the samples measured here. Samples which are highly scattering with low absorption and low quantum yield present difficulties for all fluorescent lifetime measurement technologies because of added time delay uncertainty introduced by scattering to both excitation and fluorescence photons. The lack of spectral filtering in this system will further degrade performance for such samples.

The fluorescent lifetimes of the three fluorophores were measured using the 9.5-ns pulse length because, as shown in Fig. 10, the peak power of pulses is higher for longer pulses than shorter pulses, and because the fluorescence increases during the pulse as the fluorophore impulse response is convolved with the excitation pulse.

The measured intensities for the three fluorophores are plotted as points in Fig. 12. The excitation pulse used for these measurements was measured using the same paper reflection technique as in Fig. 11 and the excitation pulse is shown in Fig. 12. Since the excitation pulse has decayed to less than 1% of its peak value by the 10 ns point on the time scale, the fluorescent lifetime is measured starting at that point. The RLD method was used to calculate lifetimes for the three fluorophores using windows from 10 to 11 ns and 11 to 12 ns. These measurements are within a third of a nanosecond of previously published values with: Cy5 was measured as

0.8 ns compared to 1 ns as reported elsewhere [4], ATTO 647 was measured as 2.0 ns as compared to ATTO TEC's reported value of 2.3 ns [12], ATTO 647N was measured as 3.2 ns as compared to ATTO TEC's reported value of 3.4 ns [13]. The measured fluorescent lifetimes are plotted in Fig. 12 as colored lines associated with each fluorophore.

The integrating windows used in the RLD calculation were determined starting with the optimization performed by Ballew and Demas that showed the highest signal-to-noise ratio from RLD is achieved with integration windows roughly twice as long as the time constant being measured when the predominant noise is shot noise from the photon emission [9]. The addition of readout noise in this system shifts the optimum to shorter window lengths and 1-ns windows were used in this calculation to ensure that the signal in the second window is above the noise floor for the shortest lifetime fluorophore.

D. Multiplexing Dyes

Finally, we demonstrated fluorescent lifetime multiplexing, the ability to distinguish fluorescence from multiple fluorophores in the same spectral window, by using mixtures of ATTO 647 and ATTO 647N. We varied the fluorescence from each fluorophore by varying the concentrations of the sixteen samples with either 0, 1, 2, or 4 μM of each fluorophore as shown in the four by four array in Fig. 13(a). Each sample was placed in the TDF and the integrated fluorescence was measured starting 3 ns after the excitation pulse, starting 5.5 ns after the pulse, and starting 8 ns after the pulse. Acquisitions were performed over 2 min with averaging of 100 measurements in the microcontroller and further averaging by a factor of 100 in the host computer.

The measured fluorescence was attributed to the two fluorophores using (8) and (9) from Section II. This fluorescence was then used to calculate the fluorophore concentrations assuming that the fluorescence is linear with fluorophore concentration. This would be the case in a system with constant excitation and emission geometry and independent fluorophores [14]. Our calculated estimate was improved by correcting for absorption of both excitation and fluorescent photons. The calculated fluorophore concentration was scaled by a factor proportional to the calculated concentration of the second fluorophore in the comparison between predicted and actual concentrations in Fig. 13. This demonstrates the correlation between measured fluorescent intensities and micromolar fluorophore concentrations.

V. Conclusion and Future Work

We have developed a novel time-domain method for distinguishing fluorescence from two fluorophores and demonstrated this method using a new TDF. Fluorescent lifetime multiplexing is widely applicable to distinguishing fluorescence in more channels than can be achieved with spectral methods alone. For whole animal in vivo imaging, the ability to perform ratiometric imaging with spectrally matched channels is particularly promising because of the possibility of removing effects from tissue absorption.

The 20-dB dynamic range of the TDF was sufficient to demonstrate fluorescent lifetime multiplexing with carefully chosen concentrations, but limits the applications of the TDF for in vitro and in vivo analysis of biomedical samples. The TDF is most useful for measuring the fluorescent lifetimes of fluorophores during development of new probes for fluorescent lifetime multiplexing or other forms of fluorescent lifetime imaging. Unlike other systems for measuring fluorescent lifetime, which require large investments in money and laboratory real estate, this system can be added to labs focusing on other aspects of probe development for occasional measurements. In addition, the circuits developed for this TDF show promise for future translation to parallel arrays of detectors on an integrated circuit.

Acknowledgments

This work was supported in part by the NIH Grants 5R01EB001872-05 “In Vivo Multichannel Fluorescent Imaging” and 5T32EB002102-26 “Postgraduate Program in Radiological Sciences.” This paper was recommended by Associate Editor S. Hu.

The authors would like to thank the reviewers for their detailed comments, which greatly improved this paper.

Biographies

Christopher D. Salthouse received the S.B., M.Eng., and Ph.D. degrees in electrical engineering from the Massachusetts Institute of Technology (MIT), Boston.

He is currently working as a Research Fellow with the Center for Molecular Imaging Research, Massachusetts General Hospital, Charlestown, where he develops new optical imaging technologies for biomedical applications. During his doctoral research with Dr. Sarpeshkar at MIT, he developed micropower analog integrated circuits to improve cochlear implants.

Ralph Weissleder is a Professor with Harvard Medical School, Director of the Center for Systems Biology, Massachusetts General Hospital (MGH), Charlestown, and an Attending Interventional Radiologist with MGH. He has been a driving force in the development of novel imaging tools and their application to understanding complex diseases. He has developed systematic ways to explore disease biology using library approaches and has been instrumental in translating several technologies into new drugs.

Umar Mahmood received the B.S. degree in chemistry from the California Institute of Technology (Caltech), Palo Alto, and the M.D. and Ph.D. degrees from Cornell University, Ithaca, NY.

He is currently an Associate Professor of Radiology with Harvard Medical School, Cambridge, MA, and Director of Small Animal Imaging with the Center for Molecular Imaging Research, Massachusetts General Hospital (MGH), Charlestown. His doctoral and postdoctoral work in biophysics were performed at Memorial Sloan Kettering Cancer Center and focused on tumor physiology studies using NMR spectroscopy. His medical residency training was in radiology at the MGH, Boston.

References

1. Giepmans BN, Adams SR, Ellisman MH, Tsien RY. The fluorescent toolbox for assessing protein locations and function. Science Apr;2006 312:217–24. [PubMed: 16614209]
2. Rao J, Dragulescu-Andrasi A, Yao H. Fluorescence imaging in vivo: Recent advances. Curr Opin Biotechnol Feb;2007 18:17–25. [PubMed: 17234399]
3. McNamara, G.; Boswell, C. Pubspectra. 2007. [Online]. Available: home.earthlink.net/~pubspectra/
4. Lifetime Data of Selected Fluorophores — Resources — ISS. Dec. 2007 [Online]. Available: www.iss.com/resources/fluorophores.html
5. Erdmann R, Kell G, Becker W, Klose EO. New Compact TCSPC Apparatus Based on Sub 15 ps Laserdiodes: Preliminary Results. Biochem Diag Instrum 1994:300–306.
6. Becker W, Bergmann A, Koenig K, Tirlapur U. Picosecond fluorescence lifetime microscopy by TCSPC imaging. Multiphoton Microscopy Biomed Sci 2001:414–419.
7. Qu J, Liu L, Chen D, Lin, Xu G, Guo B, Niu H. Temporally and spectrally resolved sampling imaging with a specially designed streak camera. Optics Lett Feb;2007 31(3):368–370.
8. Munro I, McGinty J, Galletly N, Requejo-Isidro J, Lanigan PMP, Elson DS, Dunsby C, Neil MAA, Lever MJ, Stamp GWH, French PMW. Toward the clinical application of time-domain fluorescence lifetime imaging. J Biomed Opt 2005;10:051403. [PubMed: 16292940]
9. Ballew RM, Demas JN. An error analysis of the rapid lifetime determination method for the evaluation of single exponential decays. Analytical Chem 1989;61:30–33.
10. Cubeddu R, Comelli D, D'Andrea C, Taroni P, Valentini G. Time-resolved fluorescence imaging in biology and medicine. J Phys D: Appl Phys 2002;35:61–76.
11. Akers W, Lesage F, Holten D, Achilefu S. Invivo resolution of multiexponential decays of near-infrared molecular probes by fluorescence lifetime gated whole-body time-resolved diffuse optical imaging. Molecular Imaging Aug;2007 6:237–246. [PubMed: 17711779]
12. ATTO 647. Atto-Tec Gmbh; Siegen, Germany: Mar. 2007 [Online]. Available: http://www.atto-tec.com/ATTO-TEC.com/Products/ATTO647_1.html
13. ATTO 647N. Atto-Tec Gmbh; Siegen, Germany: Mar. 2007 [Online]. Available: www.atto-tec.com/ATTO-TEC.com/Products/ATTO647N_1.htm
14. White, CE.; Argaur, RJ. Fluorescence Analysis: A Practical Approach. New York: Marcel Dekker, Inc; 1970.

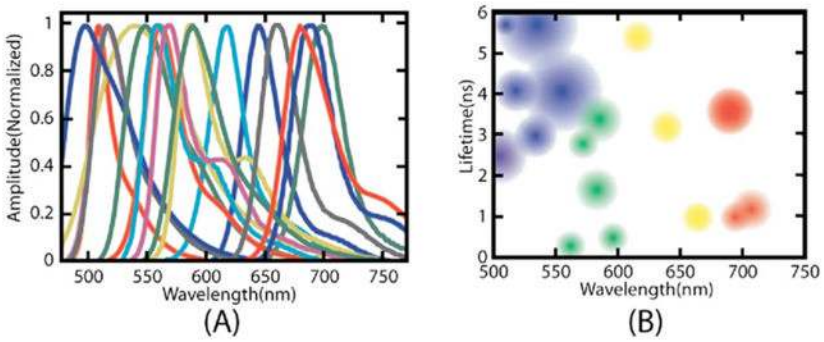

Fig. 1.

(A) Broad emission spectra of fluorophores limits the number of spectrally separated channels. (Spectra from pubspectra [3]) (B) Fluorescent lifetime can be used for additional separation to increase the number of independent channels. (Lifetimes from [4]).

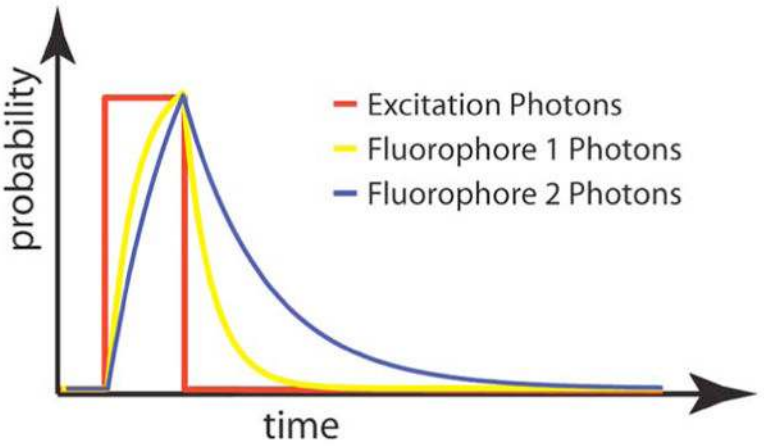

Fig. 2.

Fluorescent lifetime is a measure of the time response of a fluorophore to a pulsed excitation. The red line shows the pulse of excitation photons. The blue line is the fluorescent photons emitted from long fluorescent lifetime dye. The yellow line represents the photons from a shorter lifetime dye.

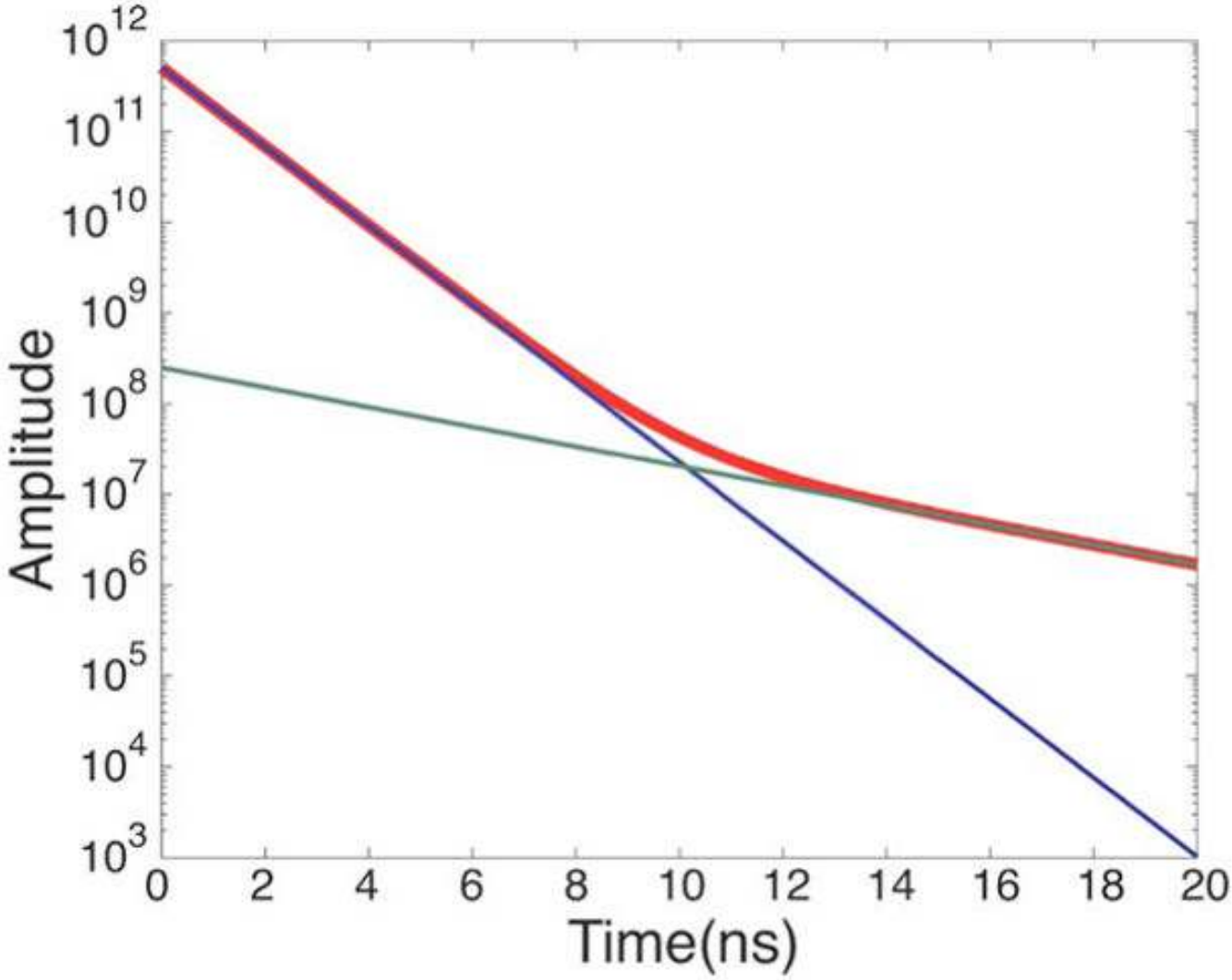

Fig. 3.

Amplitudes of two fluorophores can be measured independently given the appropriate range of fluorescent lifetimes and amplitudes. The shorter lifetime fluorophore is measured immediately following excitation. The longer lifetime dye is measured after the shorter lifetime fluorophore has decayed.

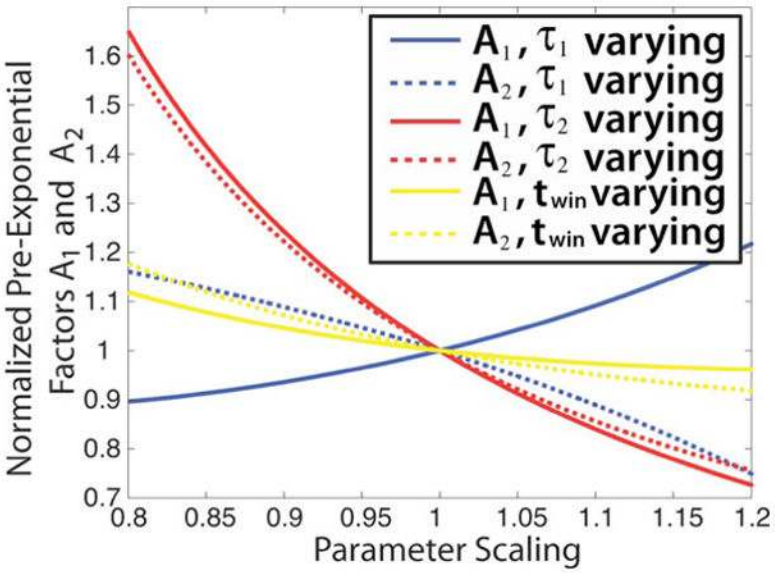

Fig. 4.

Errors in the value of the fluorescent lifetimes of the two fluorophores or in the length of the integrating time window can cause errors in calculated fluorescence from each of the fluorophores. This figure plots the calculated fluorescent intensity of two fluorophores normalized to 1 for the correct value across parameter variation from 20% below to 20% above the correct value. A low estimate of τ_2 has the greatest effect, with up to a 60% error in calculated fluorescence intensity from a 20% error in fluorescent lifetime. The other parameters cause a maximum error of less than 30% across the variation range.

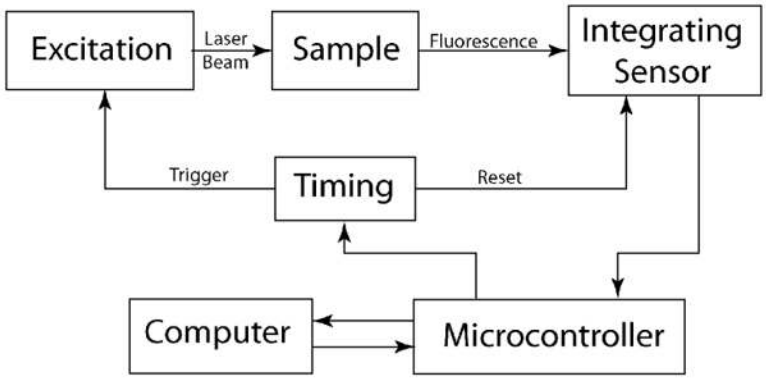

Fig. 5.
TDF is made up of five blocks. The Excitation block generates nanosecond laser pulses that pass through a sample. The integrating sensor detects the fluorescence generated in the sample. The integrator is reset at different times with respect to the excitation pulse by the timing circuit. This operation is controlled by software running on a computer through a microcontroller interface.

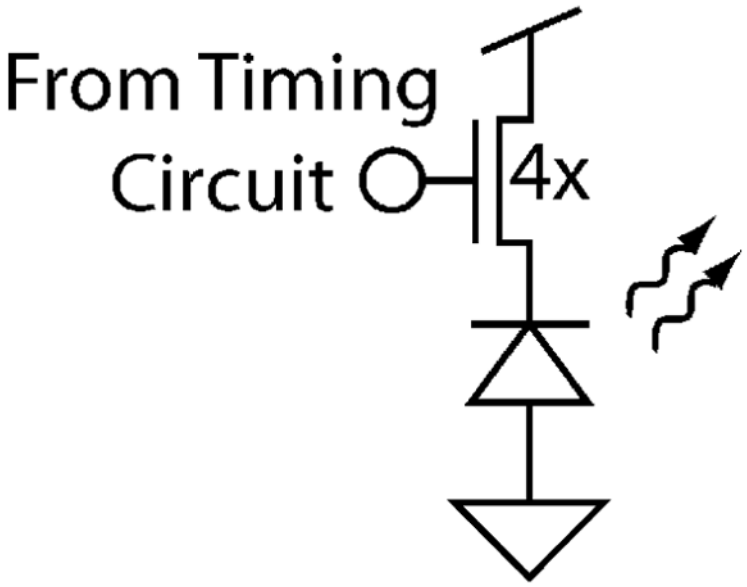

Fig. 6.
Excitation circuit uses an emitter follower configuration to drive a laser diode with nanosecond pulses.

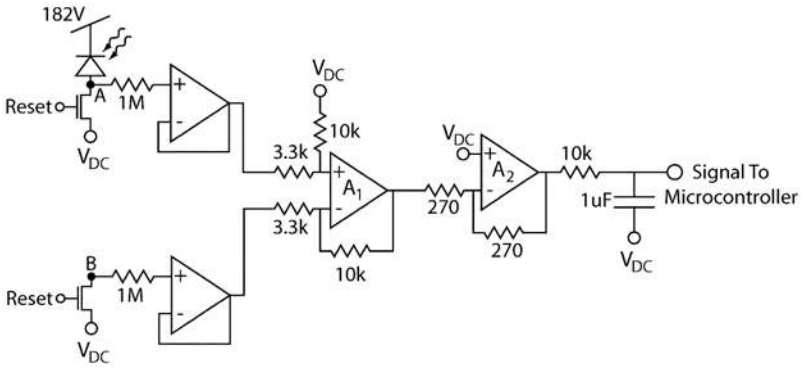

Fig. 7.

Avalanche photo diode detects and amplifies the fluorescence signal. Temporal resolution is provided by the reset switch. The signal is then buffered. A dummy signal is subtracted. The net signal is inverted and filtered before being sent to the microcontroller.

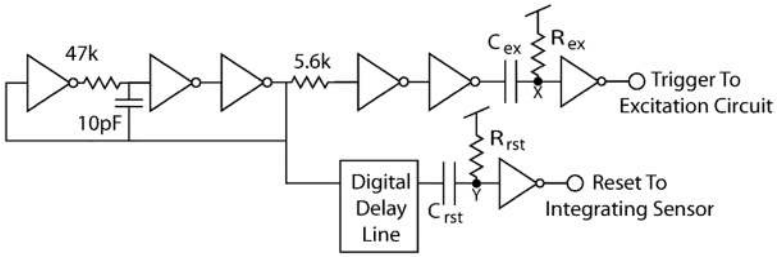

Fig. 8.

Timing circuit sends signals to the excitation and integrating sensor blocks. A three-inverter oscillator, with an *RC* delay circuit setting the oscillation frequency, forms the initial oscillation. The signal to the excitation circuit passes through a constant delay followed by an *RC* pulse shaper. The signal to the integrating sensor is delayed by programmable amounts by the digital delay line before passing through an identical pulse shaper.

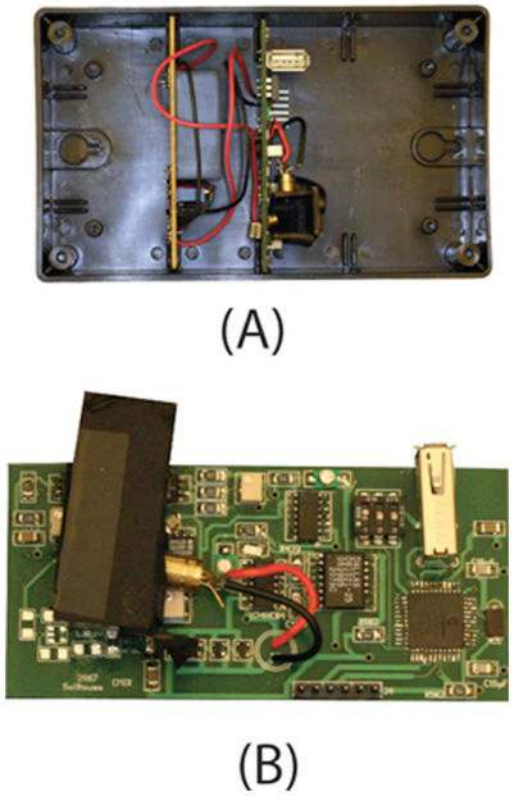

Fig. 9.
(A) System is built into a small plastic enclosure. One board holds the step up converter for the avalanche photodiode power supply. (B) The other board is a custom printed circuit board containing the remaining circuitry. The cuvette containing the sample is positioned over the sensor by the black cuvette holder.

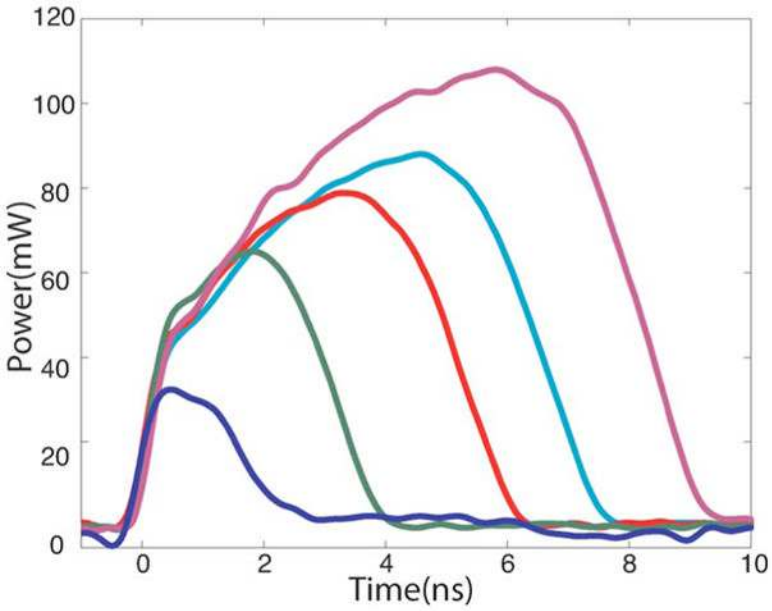

Fig. 10.
Excitation pulses were measured using a high speed photodiode and 1-GHz oscilloscope. The pulse is shown here varying from 2 to 9 ns with a peak power of over 100 mW.

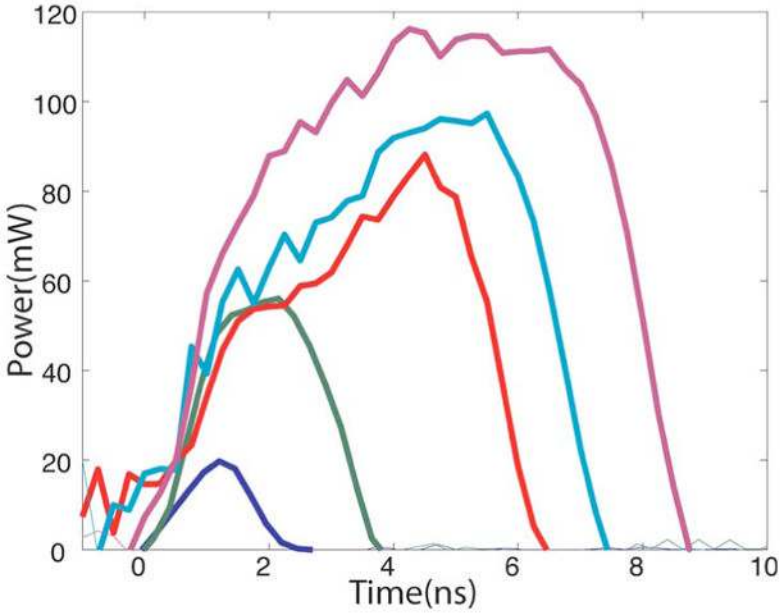

Fig. 11.

With the system configured for the same excitation pulse lengths as in Fig. 10, the excitation pulses were measured using the TDF by reflecting the excitation pulse off of a piece of white paper onto the sensor. As in Fig. 9, pulse amplitude was scaled to power based on measured average laser power.

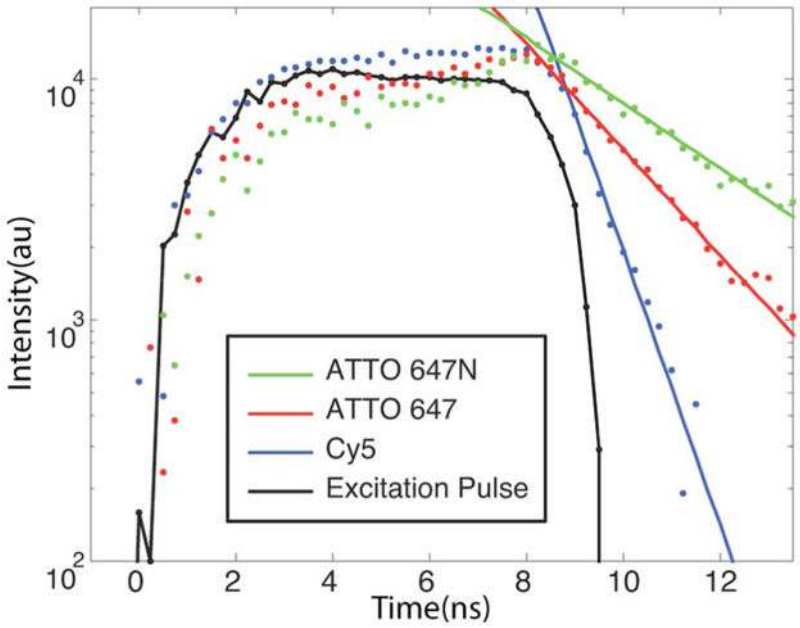

Fig. 12.

Fluorescent decay curves were measured using the TDF by adjusting the reset pulse by 250 ps steps. In this experiment, the laser excited the sample from $t = 0$ ns to $t = 9$ ns. After the excitation pulse, all three samples decayed exponentially as demonstrated by the straight lines on the semilog plot. The dots represent measurements made with the TDF. The black line connects the points of the excitation pulse. The colored lines show the slope of the fluorescent lifetimes calculated from the sampled values using RLD on windows from 10 to 11 ns and 11 to 12 ns. The calculated lifetimes were: 0.8 ns for Cy5, 2.0 ns for ATTO 647, and 3.2 ns for ATTO 647N.

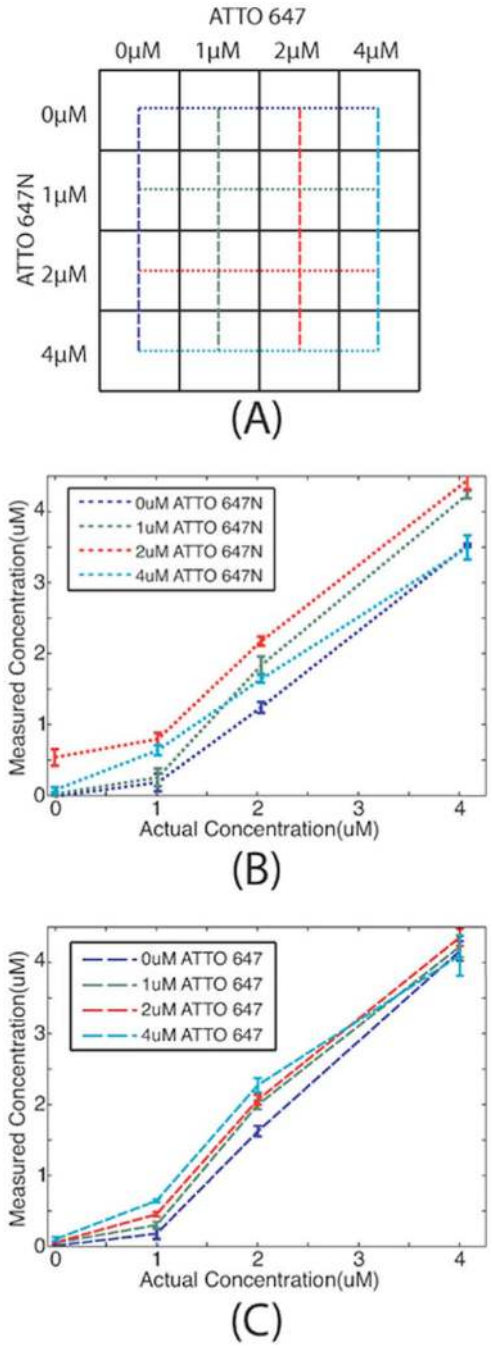

Fig. 13.

Sixteen samples were prepared by mixing various concentrations of fluorophore 1 (ATTO 647 $\tau = 2.1$ ns) and fluorophore 2 (ATTO 647N $\tau = 3.4$ ns) as shown in (A). Each combination of 0, 1, 2, and 4 μ M concentrations of each dye was measured. The measured concentrations for each of the 16 samples was then calculated. (B) shows the measured concentration of fluorophore 1 for each concentration of fluorophore 2. The lines in (B) are taken from measurements of the samples along the corresponding colored lines in (A). (C) shows the measured concentration of fluorophore 2 for each concentration of fluorophore 2, corresponding to the samples along the horizontal colored lines in (A). Three measurements were made of each mixture and standard error bars are shown.